A Statistical Approach to Dynamic Synchrony Analysis of Neuronal Ensemble Spiking

Shoutik Mukherjee and Behtash Babadi
Department of Electrical & Computer Engineering
University of Maryland, College Park, MD
E-mails: smukher2@umd.edu, behtash@umd.edu

Abstract—Neuronal ensembles have been shown to exhibit synchronized activity that is thought to be related to behavioral tasks and learning. We develop an algorithm that adaptively identifies significant synchronization of neurons based on a multivariate model of simultaneous spiking processes. We extend the statistical inference framework of adaptive Granger causal analysis to this setting in order to quantify the strength and dynamics of synchronization. We demonstrate the utility of our proposed method on simulated ensemble spiking data.

I. INTRODUCTION

Synchrony in neuronal ensembles is a phenomenon that is well-documented across many areas of the brain. The somatosensory and visual cortex of primates has been shown to exhibit synchronized stimulated responses during attentional tasks, and synchrony in the motor cortex has been shown to increase with expectation [1]. The mammalian visual pathway also demonstrates notable synchronous activity at various levels [2], [3]. This has motivated the notion of synchronous neuronal activity as a means of propagating information [4].

The study of synchrony is also closely linked to oscillatory activity, and memory and learning. Several studies have shown conditions that enable neuronal synchrony to support the cellular processes underlying learning are promoted by synchronized oscillations [5]. More recent work has shown statistical links between neural oscillations with synchrony [6].

Characterizing synchrony has largely consisted of correlational analyses of spike trains smoothed with Gaussian kernels [1], [7]. In more recent work, however, likelihood models of spike train data have been considered. The approach in [8] models ensembles with a state-space log-linear likelihood function to capture within-trial dynamics in the strength of higher-order spiking interactions. A Bayesian approach is also described to test for significant higher-order spiking. In [9] and [6], dynamic log-linear models for conditional intensity functions are used to characterize an ensemble; the log-linear components include log-probabilities of simultaneous spiking that form the basis for tests of synchrony. In [10], a multinomial Generalized Linear Model (mGLM) framework that allows the characterization of all possible simultaneous spiking events is proposed, though statistical tests for synchrony are not explored.

This work was supported in part by a University of Maryland Brain and Behavior Initiative FY18 Seed Grant award, the National Science Foundation award no. 1807216, and the National Institutes of Health award no. 1U19NS107464-01.

While the methods in [8] and [9] can capture dynamics of within-trial synchrony, they both are developed for the setting where multiple trials of an experiment were conducted and are assumed to be identical. Furthermore, in practice, limiting assumptions on the relevant higher-order interactions are required to solve the problem tractably. Conversely, the mGLM approach of [10] can be utilized to characterize all higher-order interactions during a single trial, but assumes a static underlying model and lacks an accompanying statistical framework, instead using a correlational metric to compare observed simultaneous spiking to independent interactions.

To address this gap, we propose a method to dynamically identify synchrony of all orders. Adapting recent theoretical results related to Adaptive Granger Causality (AGC) analysis [11], we also provide a framework for dynamically quantifying the significance of synchronous activity in an ensemble of spiking neurons. Applying our proposed method to simulated ensemble spiking, we demonstrate its utility in tracking the synchronous behavior of the ensemble with statistical confidence.

The remainder of this paper is organized in the following manner. In Section II, we describe an alternative representation for ensemble spiking processes and construct a joint likelihood model to capture its statistics. In Section III, we present our algorithm for identifying significant synchrony and describe the related theoretical results. In Section IV, we present and discuss our simulation studies, followed by concluding remarks in Section V.

II. PRELIMINARIES

A. Marked Process Representation of Ensemble Spiking

We model the spiking of C neurons as a multivariate process and map to a disjoint representation that allows for a convenient joint probability model. This is motivated by the modeling of ensembles with simultaneous spiking as marked point process, such as by Kass [9] and Ba [10], and its discretization as established by Ba [10]. A detailed derivation of the discrete-time model is described in [10], but we give a brief overview here.

We denote the C-variate spiking process, binned with small bin size Δ , at time t as $\mathbf{n}_t = [n_t^{(1)}, n_t^{(2)}, \dots, n_t^{(C)}]'$, where each component is the spiking process of one neuron. In our analysis, we are particularly interested in simultaneous events; however, multivariate point processes as defined in literature

1

[12] do not allow simultaneous spiking at arbitrarily small time scales. In discrete-time, this results in the modeling of spike trains as conditionally independent Bernoulli processes. The approaches in [10] and [13] directly address this shortcoming, deriving alternative representations of n_t that disjointly characterize simultaneous spiking events.

In a similar fashion, we map the spiking process n_t to a C^* -variate process $n_t^* = [n_t^{*(1)}, n_t^{*(2)}, \ldots, n_t^{*(C^*)}]'$ that are binned observations of a marked point process, where each mark counts the number of exactly one of $C^* = 2^C - 1$ disjoint non-zero outcomes of n_t . The mark space [12] is defined as $\mathcal{K} = \{1, \ldots, C^*\}$, and $n_{t_j}^*$ serves as an indicator of the mark at each time t_j such that $n_{t_j} \neq 0$. We also define the ground process $n_t^{(g)}$ that takes value 1 at each such t_j and is zero otherwise [12]; the ground process indicates the occurrence of any spiking event, and $N^{(g)} = \sum_t n_t^{(g)}$ is the total number of events. It follows from the disjointness of the marked representation that $n_t^{(g)} = \sum_{m=1}^{C^*} n_t^{*(m)}$.

Though there are many possible mappings to such a marked process, we define ours so that $n_t^{*(m)}=1$ if $n_t\neq 0$ and $m=\sum_{c=1}^C n_t^{(c)}2^{c-1}$; and $n_t^*=0$ if $n_t=0$. Note that we can recover the spiking process for the c^{th} neuron as $n_t^{(c)}=\sum_{m\in\mathcal{B}_c}n_t^{*(m)}$, where $\mathcal{B}_c=\{m=1,\ldots,C^*:m_c=1\}$ and m_c is c^{th} least significant bit of the binary representation of m. For example, suppose we have C=3 neurons; $n_t^{*(3)}$ would include spikes that occur simultaneously on only neurons $n_t^{(1)}$ and $n_t^{(2)}$, and $n_t^{(1)}=n_t^{*(1)}+n_t^{*(3)}+n_t^{*(5)}+n_t^{*(7)}$.

We define the instantaneous rates of n_t and n_t^* to be the probabilities of observing an event at time bin t. That is,

$$\lambda_t^{(c)} \Delta = \mathbb{P}[n_t^{(c)} = 1],$$

$$\lambda_t^{*(m)} \Delta = \mathbb{P}[n_t^{*(m)} = 1],$$
(1)

for $c=1,\ldots,C$ and $m=1,\ldots,C^*$. We can relate $\lambda_t^{(c)}\Delta$ to $\lambda_t^{*(m)}\Delta$ in the same manner as $n_t^{(c)}$ to $n_t^{*(m)}$, and obtain the rate of the ground process $\lambda_t^{*(g)}\Delta=\sum_{m=1}^{C^*}\lambda_t^{*(m)}\Delta$.

The marked process allows the following generative description of simultaneous spiking events: at time t, an event occurs with probability $\lambda_t^{*(g)}\Delta$; the event is assigned to the $m^{\rm th}$ mark (i.e. the $m^{\rm th}$ simultaneous spiking outcome) with conditional probability $\frac{\lambda_t^{*(m)}\Delta}{\lambda_t^{*(g)}\Delta}$. This also serves as an efficient method of generating simulated marked process data.

B. Joint Model of Simultaneous Spiking

We develop a discrete-time joint probability model based on the marked process observations n_t^* . Throughout, we assume independence across time bins. In a similar manner as [8], we define the log-linear model at time t, with parameter vector $\mu_t = [\mu_t^{(1)}, \mu_t^{(2)}, \dots, \mu_t^{(C^*)}]'$, to be

$$\log p(\boldsymbol{n}_t^*) = \boldsymbol{\mu}_t' \boldsymbol{n}_t^* - \psi(\boldsymbol{\mu}_t), \tag{2}$$

where

$$\psi(\mu_t) = \log\left(1 + \sum_{m=1}^{C^*} e^{\mu_t^{(m)}}\right) \tag{3}$$

is a normalization factor. Since each component of \boldsymbol{n}_t^* is disjoint, the log-likelihood can equivalently be written in terms of their rates as

$$\label{eq:posterior} \log \, p(\boldsymbol{n}_t^*) = \sum_{m=1}^{C^*} n_t^{*\,(m)} \log(\lambda_t^{*\,(m)} \Delta) + (1 - n_t^{(g)}) \log(1 - \lambda_t^{*\,(g)} \Delta),$$

which coincides with the likelihood defined in [10]. The m^{th} simultaneous spiking process has a rate of

$$\lambda_t^{*(m)} \Delta = \frac{e^{\mu_t^{(m)}}}{1 + \sum_{i=1}^{C^*} e^{\mu_t^{(j)}}} \tag{4}$$

and the parameters

$$\mu_t^{(m)} = \log\left(\frac{\lambda_t^{*(m)}\Delta}{1 - \lambda_t^{*(g)}\Delta}\right) \tag{5}$$

are the log-odds of the event $n_t^{*(m)}=1$ versus $n_t^{(g)}=0$. Recalling the mapping between the spiking and simultaneous spiking processes, we can find the rate of the $c^{\rm th}$ spiking process as

$$\lambda_t^{(c)} \Delta = \sum_{m \in \mathcal{B}_c} \lambda_t^{*(m)} \Delta. \tag{6}$$

We assume that over a window of length W, μ_t 's are constant. The log-likelihood of the i^{th} such window is $\ell_i(\mu_i) = W(\mu_i' \bar{n}_i^* - \psi(\mu_i))$, where $\bar{n}_i^* := \frac{1}{W} \sum_{j=(i-1)W+1}^{iW} n_j^*$. The log-likelihoods up to the k^{th} window are combined using the forgetting factor mechanism into an RLS-like objective [14] that captures dynamics in the rates of simultaneous spiking processes. That is,

$$\ell_k^{\beta}(\boldsymbol{\mu}_k) := (1-\beta) \sum_{i=1}^k \beta^{k-i} \ell_i(\boldsymbol{\mu}_k)
= (1-\beta) \sum_{i=1}^k W \beta^{k-i} (\boldsymbol{\mu}_k' \bar{\boldsymbol{n}}_i^* - \psi(\boldsymbol{\mu}_k)).$$
(7)

For each window k, we can solve the sequence of maximum-likelihood problems

$$\hat{\boldsymbol{\mu}}_k = \underset{\boldsymbol{\mu}_k}{\operatorname{arg\,max}} \quad \ell_k^{\beta}(\boldsymbol{\mu}_k). \tag{8}$$

However, this becomes intractable for larger ensembles since the dimensionality of μ_k grows exponentially with C; it is also possible that some marks will not contain any events. Thus, we define the set of indices $S = \{m \in \mathcal{K} : \sum_t n_t^*(m) > \gamma\}$ as the full support set to optimize over, for some pre-defined constant $\gamma > 0$, and treat the remaining simultaneous spiking processes as negligible due to the infrequency of their spiking. The sequence of maximum-likelihood problems then becomes

$$\hat{\boldsymbol{\mu}}_{k}^{(S)} = \underset{\boldsymbol{\mu}_{k}^{(S)}}{\operatorname{arg\,max}} \quad \ell_{k}^{\beta}(\boldsymbol{\mu}_{k}^{(S)}), \tag{9}$$

where

$$\ell_k^{\beta}(\boldsymbol{\mu}_k^{(S)}) = (1 - \beta) \sum_{i=1}^k W \beta^{k-i} \left(\boldsymbol{\mu}_k^{(S)'} \bar{\boldsymbol{n}}_i^{*(S)} - \psi(\boldsymbol{\mu}_k^{(S)}) \right).$$

The maximum likelihood estimate is obtained using the gradient descent algorithm. Note that the gradient at window k involves the weighted summation of $\bar{n}_i^{*(S)}$. We can use a simple recursion to compute this efficiently at each window.

The optimization procedure is summarized in Algorithm 1. The parameters I_{max} and κ are the maximum number of gradient-descent iterations and step size, respectively. In step 4, the term $\exp(\hat{\boldsymbol{\mu}}_k^{(S)})$ is understood to be an element-wise operation.

Algorithm 1 ML Estimation over support set S

Input:
$$\{\bar{n}_k^*\}_{k=1}^K$$
, β , S , I_{max} , κ

Output: $\{\hat{\mu}_k^{(S)}\}_{k=1}^K$

Initialization: $\mathbf{x}_0 = \mathbf{0}$, $\{\hat{\mu}_k^{(S)}\}_{k=1}^K = \mathbf{0}$

1: for $k=1$ to K do

2: $\mathbf{x}_k = \beta \mathbf{x}_{k-1} + \bar{n}_k^{*(S)}$

3: for $iter = 1$ to I_{max} do

4: $\hat{\lambda}_k^{*(S)} \Delta \leftarrow \exp(\hat{\mu}_k^{(S)}) / \left(1 + \sum_{m \in S} \exp(\hat{\mu}_k^{(m)})\right)$

5: $\nabla \ell_k^{\beta}(\hat{\mu}_k^{(S)}) = W\left(\mathbf{x}_k - \frac{1-\beta^k}{1-\beta}\hat{\lambda}_k^{*(S)}\Delta\right)$

6: $\hat{\mu}_k^{(S)} \leftarrow \hat{\mu}_k^{(S)} + \kappa \nabla \ell_k^{\beta}(\hat{\mu}_k^{(S)})$

7: end for

8: end for

9: return $\{\hat{\mu}_k^{(S)}\}_{k=1}^K$

III. CHARACTERIZING SIGNIFICANT HIGHER ORDER SYNCHRONY

Simultaneous spiking events occur by chance in an ensemble of independent neurons; however, synchronization of activity is indicative of deeper relationships between units in the ensemble. We focus on characterizing the significance of r^{th} order synchrony (i.e. r-wise simultaneous spiking), for some integer r > 2, by constructing the hypothesis test:

$$H_0$$
: r^{th} order simultaneous spikes occur as frequently as they would between independent units (10)

 H_1 : $r^{\rm th}$ order simultaneous spikes occur at a significantly higher rate than they would between independent units

In [9], similar hypotheses are formulated to examine the synchrony of one specified set of neurons. It is noted in [9] that the difference in the rate of synchronous activity is a multiplicative factor, and so this factor is used to quantify the null hypothesis and its estimate as the test statistic.

We instead quantify the null hypothesis with a nested model that assumes r^{th} order interactions are chance occurrences. First consider the subset of S that consists of the r-wise simultaneous spiking processes $S_r = \{m \in S : \sum_{c=1}^C m_c = r\}$, where, as before, m_c is the c^{th} least significant bit of the binary representation of m. The reduced model is estimated by solving the maximum likelihood problems

$$\hat{\boldsymbol{\mu}}_k^{(R)} = \underset{\boldsymbol{\mu}_k^{(R)}}{\operatorname{arg\,max}} \quad \ell_k^{\beta}(\boldsymbol{\mu}_k^{(R)}) \tag{11}$$

using Algorithm 1, where we fix $\mu_k^{(m)}$ at a base rate of $\mu_{0,k}^{(m)}$, for $m \in S_r$. The base rate of $\mu_{0,k}^{(m)}$ is the log-odds of $n_k^{*(m)} = 1$ versus $n_k^{(g)} = 0$ under the assumption that the

neurons are independent. The probabilities of each event is given, respectively, by

$$\mathbb{P}[n_k^{*(m)} = 1] = \prod_{c_a: m_{c_a} = 1} \left(\lambda_k^{(c_a)} \Delta \right) \prod_{c_b: m_{c_b} = 0} \left(1 - \lambda_k^{(c_b)} \Delta \right), \tag{12}$$

and

$$\mathbb{P}[n_k^{(g)} = 0] = \prod_{c=1}^{C} \left(1 - \lambda_k^{(c)} \Delta \right). \tag{13}$$

Evaluating each at the maximum likelihood estimate $\hat{\mu}_k^{(S)}$ and taking the ratio, we obtain

$$\mu_{0,k}^{(m)} = \sum_{c:m_c=1} \log \left(\frac{\hat{\lambda}_k^{(c)} \Delta}{1 - \hat{\lambda}_k^{(c)} \Delta} \right). \tag{14}$$

The hypotheses at time k are then quantitatively stated as

$$H_0 : \boldsymbol{\mu}_k = \hat{\boldsymbol{\mu}}_k^{(R)}$$

$$H_1 : \boldsymbol{\mu}_k = \hat{\boldsymbol{\mu}}_k^{(F)} := \hat{\boldsymbol{\mu}}_k^{(S)}$$
(15)

To test between the nested full and reduced models, we adapt recent theoretical results for AGC analysis [11] to our setting. Though classical results for nested hypothesis tests using the deviance difference test statistic $D(\hat{\mu}^{(F)}, \hat{\mu}^{(R)}) := 2(\ell(\hat{\mu}^{(F)}) - \ell(\hat{\mu}^{(R)}))$ have been established [15], [16] and are commonly used, they are ill-suited here due to the forgetting factor mechanism that exponentially weights data log-likelihoods. In a related context, this issue is addressed in [11] by defining the adaptive de-biased deviance difference and establishing its limiting distributions under both the presence and absence of Granger causal links.

Because our estimates are asymptotically unbiased, we can instead use the adaptive deviance difference

$$D_{k,\beta}^{(r)}(\hat{\boldsymbol{\mu}}_k^{(F)}, \hat{\boldsymbol{\mu}}_k^{(R)}) := 2\left(\frac{1+\beta}{1-\beta}\right) \left(\ell_k^{\beta}(\hat{\boldsymbol{\mu}}_k^{(F)}) - \ell_k^{\beta}(\hat{\boldsymbol{\mu}}_k^{(R)})\right) \tag{16}$$

as the test statistic. The limiting distributions of the adaptive deviance difference for our joint model under both the null and alternative hypotheses take similar forms as in [11]. Specifically, it can be shown that, as $\beta \to 1$,

- i) under H_0 , i.e. if r^{th} order synchrony matches independent r^{th} order interactions, $D_{k\beta}^{(r)} \xrightarrow{d} \chi^2(M^{(d)})$, and
- ii) under H_1 , i.e. if r^{th} order synchrony exceeds independent r^{th} order interactions, $D_{k\beta}^{(r)} \xrightarrow{d} \chi^2(M^{(d)}, \nu_k^{(r)})$

where $\nu_k^{(r)}$ is the non-centrality parameter at time k that depends only on the true parameters, and the degree of freedom $M^{(d)}:=|S_r|$ is the difference in the cardinalities of the full and reduced support sets. The proof of this result is omitted for brevity; it closely follows that in [11] and is based on the treatment in [17] for a sequence of local hypotheses. Fully characterizing the limiting distribution of $D_{k,\beta}^{(r)}$ under H_1 requires estimating the non-centrality parameter. We assume the parameter evolves smoothly in time and use the non-central chi-square filtering/smoothing algorithm from [11] to estimate it at each window.

We not only identify r^{th} order synchrony by testing H_0 , but also quantify the strength of the synchronization using the

limiting distribution under H_1 . The significance of r^{th} order synchrony is captured by computing the Youden's J-statistic

$$J_k := 1 - \alpha - F_{\chi^2(M^{(d)}, \hat{\nu}_k)}(F_{\chi^2(M^{(d)})}^{-1}(1 - \alpha))$$
 (17)

for significance level α . By convention, we take $J_k=0$ when H_0 is not rejected at the k^{th} window. At windows when we do reject H_0 in favor of H_1 , values of J_k closer to 1 correspond to larger non-centrality parameter values and thus a stronger indication of synchrony. The entire procedure for identifying significant r^{th} order synchrony is described in Algorithm 2.

Algorithm 2 Dynamic r^{th} Order Synchrony Analysis

```
Input: n_t, r, \beta, \alpha
Output: J_k^{(r)}, \hat{\nu}_k^{(r)}, D_{k,\beta}^{(r)}

1: Map to n_t^* from n_t

2: S = \{m \in \mathcal{K} : \sum_t n_t^{*(m)} > \gamma\}

3: S_r = \{m \in \mathcal{S} : \sum_{c=1}^C m_c = r\}

4: M^{(d)} = |S_r|

5: for k = 1 to K do

6: Estimate full model \hat{\mu}_k^{(S)} using Algorithm 1

7: Estimate reduced model \hat{\mu}_k^{(R)} using Algorithm 1

8: D_{k,\beta}^{(r)} = 2(\frac{1+\beta}{1-\beta})(\ell_k^\beta(\hat{\mu}_k^{(S)}) - \ell_k^\beta(\hat{\mu}_k^{(R)}))

9: if F_{\lambda}^{-1}(M^{(d)})(1-\alpha) < D_{k,\beta}^{(r)} then

10: h_k = 1

11: else

12: h_k = 0

13: end if

14: end for

15: Estimate \hat{\nu}_k^{(r)} via non-central \chi^2 filtering/smoothing

16: J_k^{(r)} = h_k \times (1-\alpha - F_{\chi^2(M^{(d)},\hat{\nu}_k)}(F_{\chi^2(M^{(d)})}^{-1}(1-\alpha)))

17: return J_k^{(r)}, \hat{\nu}_k^{(r)}, D_{k,\beta}^{(r)}
```

IV. SIMULATION RESULTS

We test our proposed algorithm for dynamic synchrony analysis on simulated data. The spike trains of five neurons are simulated so that the $r^{\rm th}$ order simultaneous spiking processes exhibit significant activity during each of three epochs of the simulation (r varies between epochs), though each neuron's firing rate is kept constant throughout. We also simulate five independent neurons with the same firing rates as a basis for comparison.

We apply the algorithm to the set of independent processes and the processes with higher-order interactions. The same hyperparameters are used in both settings. We set the window size over which parameters are assumed constant W=10; and the forgetting factor $\beta=0.95$. The statistical tests are performed at level $\alpha=0.05$. Figures 1 and 2 show the analysis of the neurons with higher-order interactions and the independent neurons, respectively.

The asterisks in panels A and B of both figures denote the occurrence of an event. Comparing Figures 1–A and 2–A, we note that there is no obvious difference that can be observed from the spiking processes. However, the difference is obvious from the marked point process representations. Figures 1–B and 2–B show the respective sums of the $r^{\rm th}$ order marked

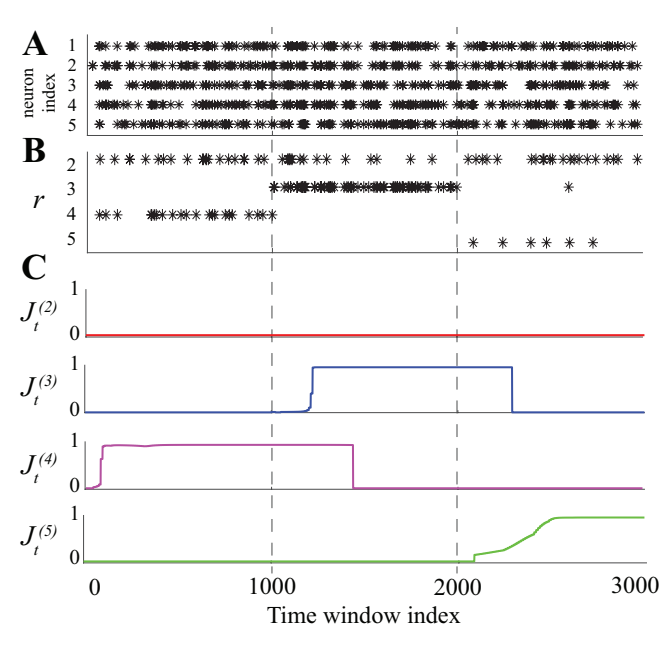


Fig. 1: Analysis of neurons with dynamic higher-order synchrony. Figure 1–A shows the spiking of five neurons with varying synchrony patterns; note that there is no obvious evidence of either synchrony or dynamics. Figure 1–B shows the sum of the $r^{\rm th}$ order marked processes for r=2,3,4,5. It is visible here that there are indeed higher-order spiking dynamics. Figure 1–C shows the time course of the J-statistics for each order. Saturation close to 1 indicate synchrony that significantly exceeds independent $r^{\rm th}$ order spiking.

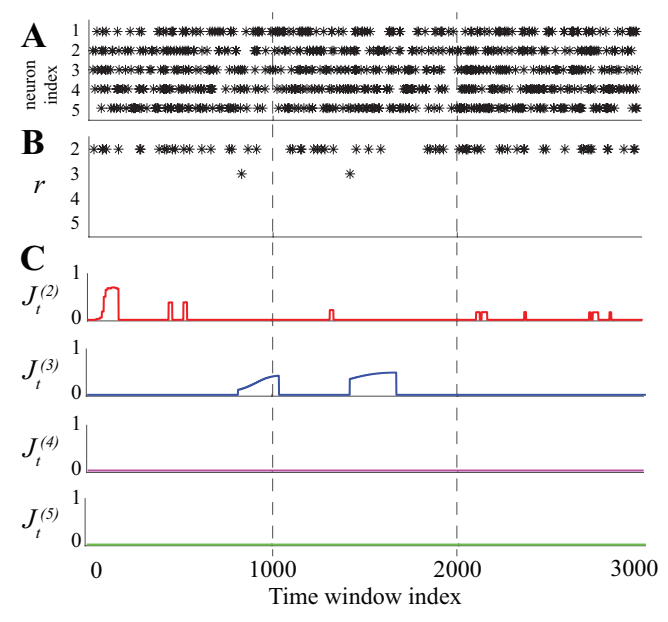


Fig. 2: Analysis of independent neurons. Figure 2–A shows the spiking of five independent neurons. Figure 2–B shows the sum of the $r^{\rm th}$ order marked process for r=2,3,4,5. There are frequent $2^{\rm nd}$ order interactions and two instances of $3^{\rm rd}$ order interactions, but no higher-order synchronization. Figure 2–C shows the J-statistics over time for each order. Though there is frequent $2^{\rm nd}$ order spiking, they occur by chance and are not indicative of deeper correlations. The J-statistic for $3^{\rm rd}$ order synchrony increases slightly for a short duration after each $3^{\rm rd}$ order event, but promptly returns to 0.

processes. This compact display of all r^{th} order spiking events allows us to clearly observe the synchrony of the spiking

activity.

The J-statistics corresponding to the $r^{\rm th}$ order synchrony is plotted in Figures 1–C and 2–C for the two settings, respectively. Amongst the independent neurons, no $4^{\rm th}$ or $5^{\rm th}$ order spiking was observed and so the $J_t^{(4)}=J_t^{(5)}=0$ throughout; the J-statistic for $3^{\rm rd}$ order synchrony increases slightly and briefly after each of the $3^{\rm rd}$ order spiking events but does not saturate close to 1, indicating weak synchronization. Amongst the neurons with higher-order interactions, the J-statistics for $3^{\rm rd}$, $4^{\rm th}$, and $5^{\rm th}$ order synchrony each saturate close to 1 and decrease in correspondence with changes in observed $r^{\rm th}$ order spiking. Note that the apparent delay in the J-statistics following the changes in each epoch is expected due to the forgetting factor mechanism utilized in capturing the dynamics.

In Figure 2–C, we do observe the J-statistic for 2^{nd} order synchrony increase at a few instances; this is preceded by pairwise spikes that occur soon after one another that our dynamic algorithm take as evidence of temporary increase in instantaneous rates. As we noted previously, since the J-statistic does not saturate close to 1, this can be interpreted as occasional weak synchronization.

Most importantly, $2^{\rm nd}$ order spiking is not registered as evidence of strong synchrony although it occurs persistently at a higher frequency. Pairwise simultaneous spikes occur by chance (or at least with the same probability as independent neurons) under both simulated conditions, and so are inherently more likely events than r>2 independent neurons spiking simultaneously. So, even though the observed probabilities of $2^{\rm nd}$ order spiking seems comparatively high, they do not significantly exceed the probability of independent pairwise spiking. This highlights the distinction between highly correlated spiking and statistically significant correlated spiking, which is clearly captured by our proposed algorithm.

V. CONCLUDING REMARKS

We develop and demonstrate an algorithm that can dynamically identify and characterize the strength of significant within-trial synchrony, addressing a current gap in similar analyses of neuronal data modeled as point processes. The application of this algorithm does not require an assumption of identically repeated trials, thus enabling dynamic analysis of synchronization in neuronal ensembles where reproducibility of exact experimental conditions and neural responses is difficult. The proposed dynamic synchrony analysis algorithm moves towards an online method of identifying synchrony that, along with similar existing methods such as AGC analysis, would form a unified framework for assessing network-level functional characteristics of neuronal ensembles.

REFERENCES

- [1] E. Salinas and T. J. Sejnowski, "Correlated neuronal activity and the flow of neural information," *Nature Reviews Neuroscience*, vol. 2, 2001.
- [2] M. Meister, R. Wong, D. A. Baylor, and C. J. Shatz, "Synchronous bursts of action potentials in ganglion cells of the developing mammalian retina," *Science*, vol. 252, no. 5008, pp. 939–943, 1991.
- [3] W. M. Usrey and R. C. Reid, "Synchronous activity in the visual system," *Annual Review of Physiology*, vol. 61, no. 1, pp. 435–456, 1999.

- [4] M. Diesmann, M.-O. Gewaltig, and A. Aertsen, "Stable propagations of synchronous spiking in cortical neural networks," *Nature*, vol. 402, 1999
- [5] M. J. Jutras and E. A. Buffalo, "Synchronous neural activity and memory formation," *Current Opinion in Neurobiology*, vol. 20, no. 2, pp. 150– 155, 2010.
- [6] P. Zhou, S. D. Burton, A. C. Snyder, M. A. Smith, N. N. Urban, and R. E. Kass, "Establishing a statistical link between network oscillations and neural synchrony," *PLOS Comput Biol*, vol. 11, pp. 1–25, 10 2015.
- [7] M. Denker, M. Diesmann, S. Grun, A. Riehle, S. Roux, and H. Linden, "The local field potential reflects surplus spike synchrony," *Cerebral Cortex*, vol. 21, pp. 2681–2695, 04 2011.
- [8] H. Shimazaki, S. ichi Amari, E. N. Brown, and S. Grun, "State-space analysis of time-varying higher-order spike correlation for multiple neural spike train data," *PLoS Comput Biol*, vol. 8, p. e1002385, March 2012
- [9] R. E. Kass, R. C. Kelly, and W.-L. Loh, "Assessment of synchrony in multiple neural spike trains using loglinear point process models," *Ann. Appl. Stat.*, vol. 5, pp. 1262–1292, 06 2011.
- [10] D. Ba, S. Temereanca, and E. N. Brown, "Algorithms for the analysis of ensemble neural spiking activity using simultaneous-event multivariate point-process models," *Frontiers in Computational Neuroscience*, vol. 8, no. 6, 2014.
- [11] A. Sheikhattar, S. Miran, J. Liu, J. B. Fritz, S. A. Shamma, P. O. Kanold, and B. Babadi, "Extracting neuronal functional network dynamics via adaptive granger causality analysis," *Proceedings of the National Academy of Sciences*, vol. 115, no. 17, pp. E3869 E3878, 2018.
- [12] D. J. Daley and D. Vere-Jones, An Introduction to the Theory of Point Processes, vol. 1. New York, NY: Springer, 2nd ed., 2003.
- [13] V. Solo, "Likelihood functions for multivariate point processes with coincidences," in *Proceedings of IEEE Conference on Decision and Control*, vol. 3, pp. 4245 – 4250, 2007.
- [14] S. S. Haykin, Adaptive Filter Theory. Upper Saddle River, NJ: Prentice Hall, 1996.
- [15] S. S. Wilks, "The large-sample distribution of the likelihood ratio for testing composite hypotheses," *Ann. Math. Statist.*, vol. 9, no. 1, pp. 60– 62, 1938.
- [16] A. Wald, "Tests of statistical hypotheses concerning several parameters when the number of observations is large," *Transactions of the American Mathematical Society*, vol. 54, no. 3, pp. 426–482, 1943.
- [17] R. R. Davidson and W. E. Lever, "The limiting distribution of the likelihood ratio statistic under a class of local alternatives," *Sankhya: The Indian Journal of Statistics, Series A (1961-2002)*, vol. 32, no. 2, pp. 209–224, 1970.